Effect of Cold Start on Engine Performance and Emissions from Diesel Engines Using IMO Compliant Distillate Fuels

Thuy Chu Van[1a, 2], Ali Zare[3], Mohammad Jafari[1b], Timothy A. Bodisco[3], Nicholas Surawski[4], Puneet Verma[1b], Kabir Suara[1a], Zoran Ristovski[1b], Thomas Rainey[1a], Svetlana Stevanovic[3], Richard J. Brown[1a, *]

[1a]Biofuel Engine Research Facility (BERF) –

[1b]International Laboratory for Air Quality and Health (ILAQH) –

Queensland University of Technology, 2 George St, Brisbane City, Queensland, 4000, Australia

[2]Vietnam Maritime University, 484 Lach Tray St, Hai Phong City, 180000, Vietnam

[3]Deakin University, 75 Pigdons Road, Waurn Ponds, VIC 3216, Australia

[4]University of Technology Sydney, 81 Broadway, Ultimo NSW 2007, Australia

***Corresponding Author**

Richard J. Brown, Biofuel Engine Research Facility, Queensland University of Technology (QUT), QLD 4000, Australia;

Email: richard.brown@qut.edu.au (Richard J. Brown); z.ristovski@qut.edu.au (Zoran Ristovski);

thuy.chuvan@qut.edu.au, chuthuy.vimaru@gmail.com (Thuy Chu Van);

Tel: +61 7 3138 5157; +61 7 3138 1129;

Fax: +61 7 3138 1516

HIGHLIGHTS

- Changes in injection strategy have strong effects on NO_x and $PM_{1.0}$ emissions;
- Engine coolant temperature resulted in the changes in engine injection strategy;
- CO and particles emitted significantly during the first 20 seconds of cold start;
- Fuel sulphur content was associated with an increase in particulate matter emissions;
- In coastal areas and ports, auxiliary engines significantly contributed to emissions.

GRAPHICAL ABSTRACT

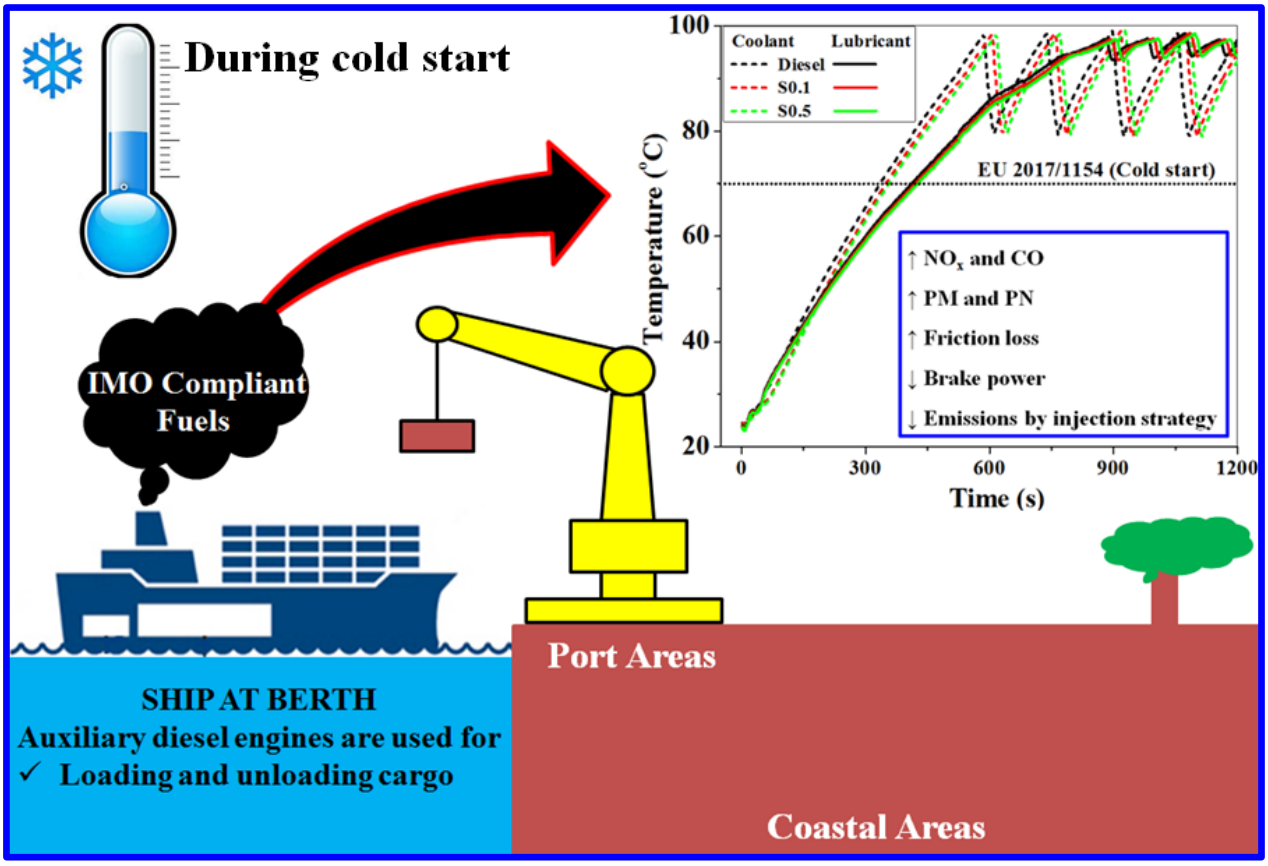

Abstract

Emissions from ships at berth are small compared to the total ship emissions; however, they are one of main contributors to pollutants into the air of densely-populated areas consequently affecting on public health heavily. This is due to auxiliary marine engines being used to generate electric power and steam for heating and providing services. The present study has been conducted on an engine representative of a marine auxiliary, which was a heavy duty, six-cylinder, turbocharged and after-cooled engine with a high pressure common rail injection system. Engine performance and emission characterisations during cold start are the focus of this paper, since cold start is significantly influential. Three tested fuels were used, including the reference diesel and two IMO (International Maritime Organization) compliant spiked fuels. The research engine was carried out at a constant speed and 25% load condition after 12 hours cooled soak. Results show that during cold start, significant heat generated from combustion is used to heat the engine block, coolant and lubricant. During the first minute compared to the second minute, emissions of particle number (PN), carbon monoxide (CO), particulate matter (PM), and nitrogen oxides (NO_x) were around 10, 4, 2 and 1.5 times higher, respectively. The engine control unit (ECU) plays a vital role in reducing engine emissions by changing the engine injection strategy based on the engine coolant temperature. IMO compliant fuels, which were higher viscosity fuels associated with high sulphur content, resulted in an engine emission increase during cold start. It should be taken into account that auxiliary marine diesel engines, working at partial load conditions during cold start, considerably contribute to emissions in coastal areas. It shows a need to implement practical measures, such as engine pre-heating, to obtain both environmental and public health advantages in coastal areas.

Key words: IMO regulations, Cold start emissions, Net of heat release rate, Engine injection strategy, Marine

auxiliary diesel engine.

1. Introduction

Cold start is defined by the Commission Regulation European Union (EU) 2017/1154 as the period of time from the first start of the engine (after minimum soak time of 12 hours, or 6 hours with forced cooling) until its coolant temperature has reached 343 K (70 °C). During cold start, the main engine block, engine coolant and lubricant temperature are low, being similar to that of the ambient air temperature and consequently sub-optimal for engine combustion, resulting in higher amount of fuel consumed and higher engine emissions (Roberts et al., 2014; Zare et al., 2018). Moreover, increasing of friction losses and decreasing of indicated thermal efficiency have been observed at low temperatures with subsequent higher lubricant viscosity (Roberts et al., 2014). A previous study also found that a cold engine block condition results in uncompleted combustion, consequently affecting engine emissions (Cao, 2007). Similarly, a recent study found that during cold start engine friction losses are three times higher than that of a warmed-up engine (Will and Boretti, 2011). These authors also stated that in order to maintain engine brake output power and to compensate for high friction losses during cold start, a greater quantity of fuel injection is needed. This is, during cold start, in agreement with another study showing a 13.5% rise in engine brake specific fuel consumption, compared to engine operation during hot start condition (Samhaber et al., 2001).

Cold start condition-related engine emissions significantly contribute to total engine emissions (Arumugam Sakunthalai et al., 2014; Reiter and Kockelman, 2016; Zare et al., 2018). A previous report showed that over 40% of total emissions of diesel engines were associated with the first three minutes of operation (Bielaczyc et al., 2001). A recent study by Chen et al. (2017) showed that more than 50% of total particulate matter (PM) and particle number (PN) emissions from a standard driving cycle, the New European Driving Cycle (NEDC), was related to Phase 1 which is cold start. Marine auxiliary engines, compared to NEDC engines, normally experience the sudden and large load changes during loading and unloading cargo conditions when the ship is at berth. Therefore, it is believed that cold start emissions can account for a significant proportion of total marine engine emissions. In addition, a remarkable portion of daily driving starts and stops when the engine block temperature is still lower than its normal operation (Reiter and Kockelman, 2016). In actual fact, engine operation during cold start, an unavoidable fraction of the daily driving timetable, can remarkably contribute to a high portion of vehicles in highly-dense population areas such as cities (André, 1991). However, almost all of previous research have only concentrated on engine operation during hot start (Zare et al., 2017).

Shipping is evaluated as one of the most fuel-efficient modes of global transportation, compared to other forms of transport (Corbett, 2003). It accounts for over 80% of global trade and is forecasted to increase in the coming years (IMO, 2009; United Nations, 2017). However, exhaust emissions emitted from marine diesel engines have harmful impacts on the environment and consequently on human health. As such, they have become of international issue over the last years (Anderson et al., 2015; Blasco et al., 2014; Corbett et al., 2007; Di Natale and Carotenuto, 2015; Mueller et al., 2015; Reda et al., 2015; Ristovski et al., 2012; Winnes et al., 2016). Over 70% of emissions from ships may be measurable up to 400 km inshore and have a significant contribution to an increase in concentrations of particulate matter as well as of gaseous pollutants in areas closer to harbours

(Eyring, 2005; Eyring et al., 2010). Although emissions from marine engines at berth account for only a relatively small portion of the total ship emissions, at-berth emissions have some of the most considerable health impacts on the surrounding environment because of their proximity to areas of high population density (Cooper, 2003; Winnes and Fridell, 2010). While the ship is at berth, generally only the auxiliary marine engines and economisers are in operation to generate electric power and steam for heating and providing services (Chu-Van et al., 2017). Moreover, the difference between auxiliary and main marine diesel engines is that main marine diesel engines are always pre-heated before running, while auxiliary engines are typically started cold. It shows that auxiliary engines during cold start exacerbate the port emission issue, as they are mostly ultilised during ship harbour stopovers. In addition, once running, auxiliary engine load conditions continuously vary in a wide range of 30-3000 kW depending on the ship activity, especially while loading and unloading cargo (Cooper, 2003). In this case, auxiliary engines normally experience unsteady or transient conditions, which are believed to promote engine emissions (Zare et al., 2018). However, this study does not examine transient conditions.

The International Maritime Organization (IMO) is a specialised branch of the United Nations (UN) which issues global regulations on the safety, security and environmental performance of global shipping. In particular, Annex VI of the International Convention for the Prevention of Pollution from Ships – the Marine Pollution Convention – MARPOL was adopted by the 1973 Convention, and then modified by the 1978 Protocol with regard to limit the harmful impacts of emissions from ships on air quality (IMO, 1997). These regulations were effective on 19th May 2005 to reduce nitrogen oxides (NO_x), sulphur oxides (SO_x) and PM from marine engines. These regulations control the sulphur (S) content of marine fuels to 0.1% (by mass) in Emission Control Areas (ECAs) by 2015 and to 0.5% globally by 2020 (Chu Van et al., 2019). The reduction in $PM_{2.5}$ emissions (by mass) is a result of using low S fuels (Sofiev et al., 2018). This study stated that cleaner marine fuels by 2020 will significantly contribute to the reduction of global ship-related morbidity and premature mortality by 54 and 34%, respectively. However, marine fuels with lower S content will still significantly contribute to the number of annual related fatalities (~250,000 deaths) as well as ~6.4 million cases of childhood asthma. Therefore, more studies related to IMO compliant fuels are necessary in order to understand ship emission characteristics more thoroughly.

Based on a review of the relevant literature related to ship emissions, there are no similar publications on ship emission measurements during cold start using IMO compliant fuels. In the present study, test-bench measurements were carried out on a marine auxiliary, heavy duty, six-cylinder, turbocharged and after-cooled diesel engine with a high pressure common rail injection system with regard to investigate engine performance and emission characterisations during cold start. The research engine was examined at a constant speed (1500 rpm) and 25% load condition under engine cold start conditions (after 12 hours cooled soak). The fuel S contents were selected related to the current and up-coming IMO regulations.

2. Methodology

2.1. Tested engine specification

This experimental investigation used a heavy duty, six-cylinder, turbocharged, after-cooled diesel engine with a high pressure common rail injection system located in the Biofuel Engine Research Facility (BERF) at Queensland University of Technology (QUT). This engine is consistent with marine auxiliary diesel engines; however, it is not marinised. The engine was coupled to an electronically controlled water brake dynamometer which controls the engine load conditions. Fuel flow rate in litres per minute (LPM) and intake air flow rate in kg s^{-1} were measured at 1 Hz from the CAN-Bus, while the flow rate of exhaust gas was calculated from these two above-measured flow rates. The CAN-bus (the controller area network bus) is the current interface to engine operation data transmitted between engine control units (ECU). An analogue-to-digital converter (Data Translation DT9832) received the signals from an in-cylinder combustion pressure transducer (Piezoelectric Transducer, Kistler 6053CC60, with -20 pC bar^{-1} manufacturer stated sensitivity), crank angle sensor (Kistler type 2614, manufacturer stated resolution of 0.5 crank angle degrees) and engine fuel injection. A commercial blow-by sensor was used to measure engine blow-by flow rate in LPM sampled at 1 Hz from the engine crankcase. Table 1 illustrates the main test research engine specification information. Further information of the engine specifications can be seen in previous studies (Bodisco and Brown, 2013; Hossain et al., 2017; Mitchell et al., 2017; Surawski et al., 2014; Zare et al., 2017).

Table 1. Tested research engine specifications

Item	Specification
Model	Cummins ISBe220 31
Cylinders	6 in-line
Capacity (L)	5.9
Bore x Stroke (mm)	102 x 120
Maximum Torque	820 Nm @ 1500 rpm
Maximum Power	162 kW @ 2500 rpm
Compression Ratio	17.3:1
Aspiration	Turbocharged (waste gated) & after cooled
Injection Type	High pressure common rail
Dynamometer Type	Electronically controlled water brake dynamometer
Emission Standard	Euro IIIA

Fig. 1 presents the schematic diagram of the experimental set-up. The first sampling point was used for raw exhaust measurements by a Testo 350 Portable Emission Analyser for gaseous concentration including sulphur dioxide (SO_2), NO_x, carbon monoxide (CO), carbon dioxide (CO_2), oxygen (O_2), and unburned hydrocarbons (HCs). The raw hot exhaust gas was sampled directly to the DMS 500 Fast Particulate Spectrometer (Cambustion, Cambridge, UK) dilution systems (2-stage dilution systems) from the second sampling hole. In

particular, raw exhaust was first diluted with hot air at a temperature of 150 ºC and at a fixed dilution ratio (DR) of 5. The diluted sample was then transferred to the second dilution stage via a heated sampling line to prevent condensation of water and volatile organic compounds (VOCs). The secondary dilution stage was a high ratio rotating disc diluter with a DR range of 20-500. A DMS 500 was used to measure particle number size distributions in the size range of 5 nm – 1.0 µm with a sample frequency of 1 Hz. CAI (California Analytical Instruments) NO_x and CO_2 analysers also operated from the second sampling point. The third sampling point was firstly diluted through the dilution tunnel and then divided into two paths. The first path was used for a DustTrak™ II Aerosol Monitor 8530 (TSI Incorporated, Minnesota, USA), which is a light-scattering laser photometer giving real-time aerosol mass readings, was used to measure mass concentrations of PM_{10}, $PM_{2.5}$, and $PM_{1.0}$. The other path was used for a Sable CA-10 carbon dioxide analyser. More detailed descriptions of measurement instrumentation can be found in previous studies (Chu-Van et al., 2018a; Chu-Van et al., 2018b).

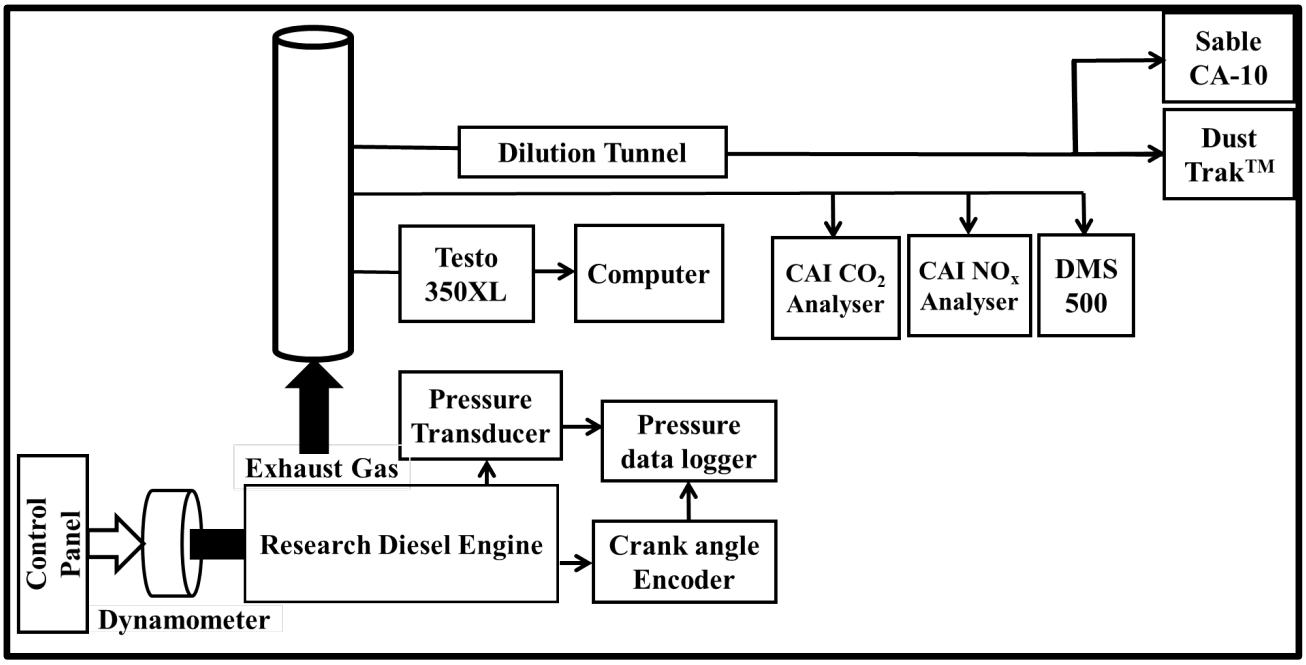

Fig. 1. Schematic diagram of experimental set-up

2.2. Fuel preparation

Three fuels were tested in the present experiment and their fuel properties are shown in Table 2. The focus of the present study is investigating the effect of fuel S contents. Selected fuel S contents were 0.1% and 0.5% (by mass), related to S regulations issued by IMO applying in ECAs by 2015 and globally by 2020, respectively. The S-species in diesel and heavy fuel oil (HFO) are not expected to be the same because of the large differences in the volatility of these two distillation cuts. The literature is not clear on the exact distribution of specific S-species in this case. However, as a compromise and for chemical simplicity, dibenzothiophene, a typical S-containing compound found in both diesel and HFO, has been selected in the present study. A detailed explanation for selecting this S-containing compound can been seen in a previous

study (Chu-Van et al., 2018a). Vanadium (V) and iron (Fe) are the common trace metals in HFO and are also un-regulated by IMO. Nevertheless, S is the priority of this research, so the fuel V and Fe contents were chosen and kept constant at 15 and 10 ppm, respectively for the two spiked fuels. It should be noted that the reference diesel fuel was not spiked with V and Fe. Further details about these metal contents can be found in a previous study (Chu-Van et al., 2018a). Chemicals containing S, V and Fe contents including dibenzothiophene, bis(cyclopentadienyl)vanadium (II) and ferrocene, therefore, have been purchased and used to spike the diesel in order to make its chemical composition similar to HFO. It is proposed that spiking diesel in this way enables the physico-chemical properties of HFO combustion to be mimicked in a marine engine. A detailed fuel quality certificate of the reference distillate diesel can be seen in the Supporting Information (Fig. S1).

Table 2. Properties of spiked fuels

Parameters	Units	Methods	Diesel	S0.1	S0.5
Density at 15 °C	kgL^{-1}	ASTM D4052	0.838[a] 0.844[b]	0.847[b]	0.85[b]
Viscosity at 40 °C	mm^2s^{-1}	ASTM D445	2.66[a] 2.66[b] 2.66[c]	3.13[c]	3.35[c]
Lubricity	mm	IP 350	0.412[a]	-	-
Carbon (C)	% mass	-	87.103[b]	88.715[b]	86.249[b]
Nitrogen (N)	% mass	-	0.054[b]	0.041[b]	0.039[b]
Sulphur (S)	% mass	ASTM D7111	$6.1x10^{-4}$[a] $7.8x10^{-4}$[b]	0.095[b] 0.093[c]	0.513[b] 0.512[c]
Vanadium (V)	$mgkg^{-1}$	ASTM D7111	<1[c]	13[c]	14[c]
Iron (Fe)	$mgkg^{-1}$		<1[c]	8[c]	8[c]
HHV*	$MJkg^{-1}$	ASTM D240	45.64[b]	44.31[b]	43.68[b]

([a] from CALTEX, [b] tested at QUT; [c] tested at Hasting Deering; * Higher heating value)

2.3. Experimental procedure

The cold start experiments were carried out in the present study after an overnight engine-off time (a minimum of 12 hours soak). The engine speed of 1500 rpm was chosen to correspond to a typical auxiliary marine engine speed. Engine load of 25% was selected since the study's priority is to investigate the effect of the engine body temperature during cold start on engine performance and emissions, but not for the engine load impact. During the test, after each fuel shift, fuel line system was thoroughly cleaned by flushing for 30 minutes with the next day's test fuel. This way, the next day's test fuel will be available in the engine fuel system and be ready for the next experiment. Several preliminary tests have been done to confirm that 30 minutes are sufficient to remove all traces of the previous fuel. However, the switching fuel time from HFO to marine gas oil (MGO) before approaching ECAs may vary greatly for the actual ship engine fuel systems. The measured engine performance and emission results were analysed within the first 120 s (2 minutes) of the cold start period. It is believed that during this period both engine performance and emissions behave totally differently compared to other one. Each test fuel was repeated three times and the variability of the results quantified by standard deviation calculations. The error analysis for the test repeatability is presented in the Supporting Information

(Tables S1, S2 and S3). The engine performance and emission results in the graphs herein are representative of averaged values.

3. Results and Discussion

3.1. Engine performance during cold start

The main focus of the test was to look at the cold start impacts on engine performance and engine emissions. The constant engine speed of 1500 rpm and engine load of 25% were maintained in order to see the effect during the cold start period. In particular, for each test, the research engine was started after an over-night soak and immediately adjusted to obtain the target speed and load as can be seen in Fig. 2a. During cold start the engine speed, along with the amount of fuel injected, were kept constant, however engine brake power gradually increased. This may be due to the increase in engine temperature resulting in friction loss decrease and improved engine thermal efficiency. This will help to increase engine torque and output power. In the literature, it is reported that a large proportion of total emissions is normally generated within the first minutes of cold start (Bielaczyc et al., 2001). So in the present study, engine performance and emissions were thoroughly analysed in the first two minutes of cold start. Figs. 2b, 2c and 2d show the coolant and lubricant temperature increasing gradually from engine start until stable values are attained. It can be seen in Fig. 2a, the temperature rise rate for both coolant and lubricant are slightly higher for reference diesel use, compared to spiked fuels use. This may be due to a small difference in ambient temperature owing to weather conditions and the calorific value of the tested fuels. In addition, the coolant temperature rise rate is significantly higher than that of lubricant, which is observed for all tested fuels. Temperatures of coolant and lubricant are the variables used by the engine management system and are controlled by thermostat in order to maintain the coolant and lubricant temperatures in the range of 80-98 ºC, and 95-98 ºC, respectively.

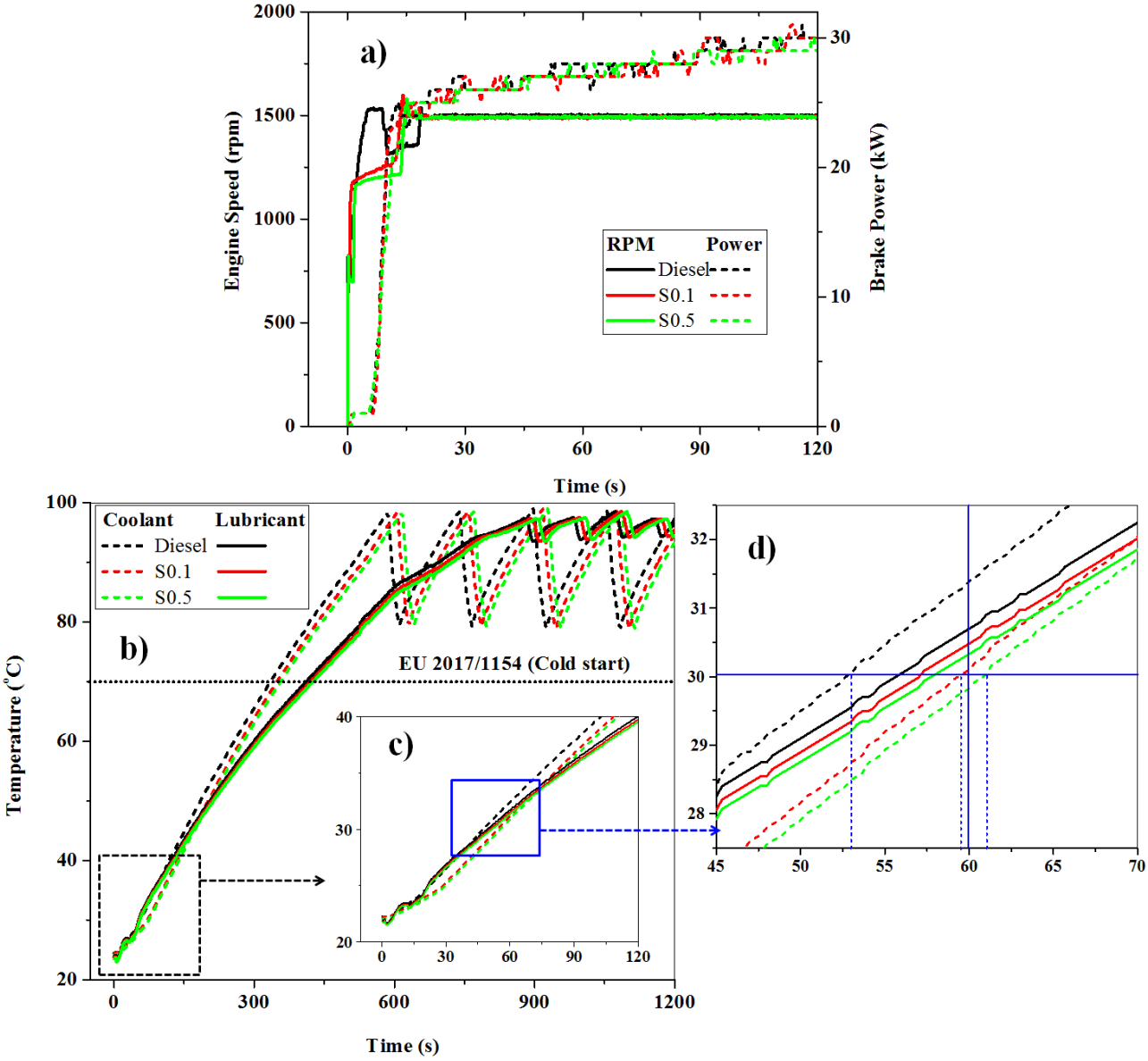

Fig. 2. a) Custom test designed for this study; b, c, d) Coolant and lubricant temperature during cold start

Figs. 3a and 3b show the in-cylinder pressure for reference diesel and IMO compliant fuels. In-cylinder pressure was averaged for every 20 s (250 cycles) in the first two minutes during cold start. It means that there are 6 different in-cylinder pressure values, which are nominated as 10, 30, 50, 70, 90 and 110 s, respectively; during the first 120 s cold start period. The reference diesel represents a higher value of in-cylinder combustion pressure than that of the spiked fuels. This is mainly due to the higher calorific value of diesel, compared to spiked fuels, which can be seen in Table 2.

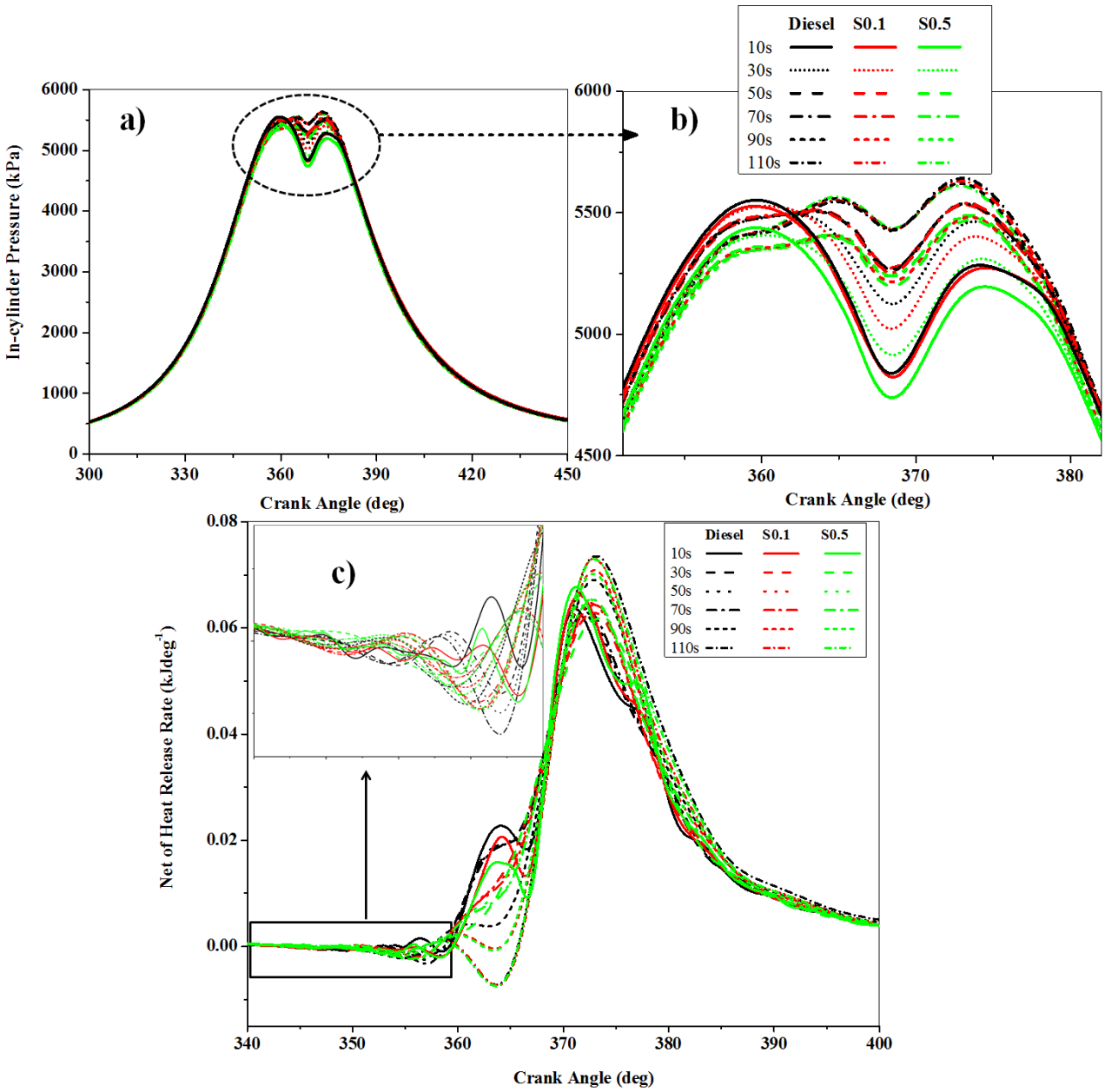

Fig. 3. a, b) In-cylinder pressure; c) Rate of heat release curves for reference diesel and IMO compliant fuels during cold start during cold start.

Fig. 3c shows the rate of net heat release curves (HRR) for different tested fuels during cold start. The HRR for 10, 30 and 50 s behave notably different to the others, which are observed for all tested fuels. This may be due to the influence of the pilot/main injection (for 10, 30 and 50 s) compared to single injection (for 70, 90 and 110 s) as can be seen in Fig. 4. Another trend with respect to HRR observed for all tested fuels is that an increase in HRR corresponds to an increase in temperatures of engine block, engine coolant and lubricant. This may be due to the heat losses for transmitting to cylinder liner decreasing along with the increasing of engine block and coolant temperature. Higher engine thermal status results in better air and fuel mixture formation, which can improve the quality of engine combustion.

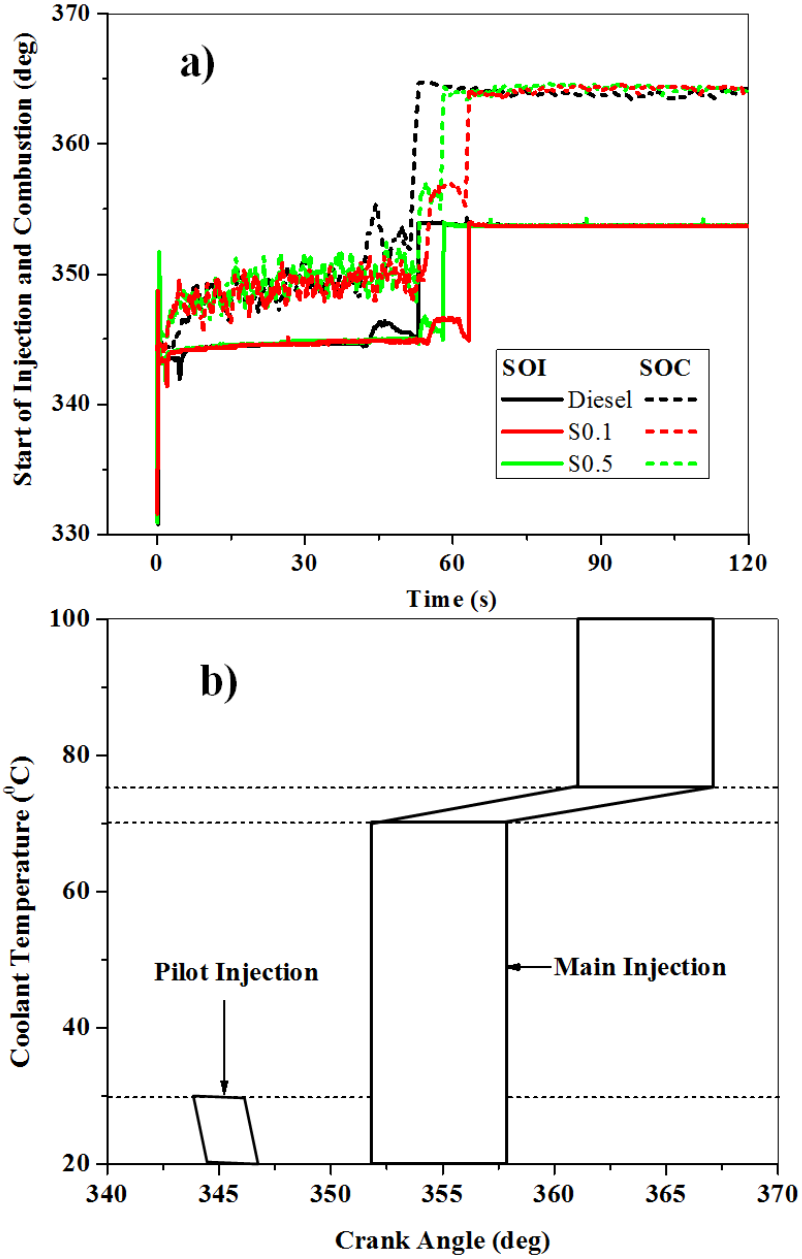

Fig. 4. a) Start of injection (SOI) and start of combustion (SOC) during cold start; b) Engine injection strategy and coolant temperature relationship

The changes in shape of in-cylinder combustion cylinder pressure curves observed in Figs. 3a and 3b are consistent for all tested fuels during the first 2-minute cold start. Normally, as the engine block and coolant temperature get warmer, the charge air loses less heat to the cylinder walls, resulting in higher in-cylinder pressure. The abnormal trend in in-cylinder pressure curves was observed at 10, 30 and 50 s compared to 70, 90 and 110 s. This can be explained by start of injection (SOI), start of combustion (SOC), and engine injection strategy, which are presented in Figs. 4a and 4b. The SOI was determined through direct interrogation of the differential voltage applied to the injector of the first cylinder and meta-heuristic parameter optimisation was used to data-fit a model against the band-pass filtered in-cylinder pressure signal to determine the SOC. This technique identifies the point at which the combustion chamber resonance commences and hence combustion

itself. During combustion the chamber is acoustically excited, this acoustic excitation causes fluctuations in the measured pressure signal. The onset of these fluctuations has been used to find the start of combustion using the accurate Bayesian method (Bodisco et al., 2013). A key advantage of using the band-pass filtered in-cylinder pressure signal for the determination of the SOC is that there is no requirement to differentiate the signal. At the point of combustion, in-cylinder pressure signals are often noisy and differentiation exasperates this, complicating any analysis including the determination of SOC. Further details about the determination of both SOI and SOC can be found in Bodisco et al. (2013). Based on the engine coolant temperature, ECU automatically adjusts the fuel injection strategy during cold start. In particular, as the engine coolant temperature is less than 30 ºC, there is both pilot and main injection, but the engine changes injection mode from pilot/main to single injection when the engine coolant is 30 ºC. ECU continuously changes injection timing (from 352 to 362 deg) when engine coolant is 70 ºC, as can be seen in Fig. 4b. It should be noted that it took around 350 s for the engine coolant to get 70 ºC (Fig. 2b), while SOI and SOC data shown in Fig. 4a were within the first 2 min (120 s). The reasons for the observed engine injection changes may be due to engine manufacturer optimisation aiming to reduce engine emissions and/or to limit the maximum in-cylinder pressure (preventing mechanical stress). The time that ECU changes fuel injection mode (from pilot/main to single injection) is different for particular tested fuels, as can be seen in Fig. 4a. The fuel injection mode started to change at the 53rd, 59th and 62nd second during the first 2-minute cold start for reference diesel, S0.1 and S0.5, respectively. These values can be seen clearly in Fig. 2d, which also shows that the corresponding coolant temperature was 30 ºC in each case at this point.

3.2. Engine emissions during cold start

Figs. 5a and 5b reveal CO and NO_x emissions during cold start for different tested fuels. It is obvious that during cold start, the main engine block, temperatures of engine coolant and lubricant are sub-optimal for combustion, resulting in higher engine emissions. All of the tested fuels show the highest CO emissions during the first 20 s of cold start. However, fuels with higher sulphur content emitted higher CO than that of the reference diesel. This is most likely due to differences in fuel viscosity, in which higher viscosity values were measured for the spiked fuels (Table 2) and/or different fuel chemical characteristics. A combination of lower engine block temperature and higher fuel viscosity make CO emissions the highest value for S0.5. This should be taken into consideration, since IMO compliant fuels will be widely used for both main and auxiliary diesel engines, especially in harbour areas. The emission of NO_x is greatly determined by temperature of engine combustion chamber. NO_x emissions observed in Fig. 5b show a gradual increase along with increasing engine cylinder liner and coolant temperature. However, a sudden drop in NO_x emissions may be attributed to the effect of the ECU strategy based on coolant temperature, which changed the fuel injection mode from two injections (pilot and main injection) to single injection. The pilot injection heats the engine combustion chamber prior to the main injection. This in turn creates hotter combustion of the fuel injected in the main injection. Therefore, more thermal NO_x emissions were emitted during the pilot and main injection period of time.

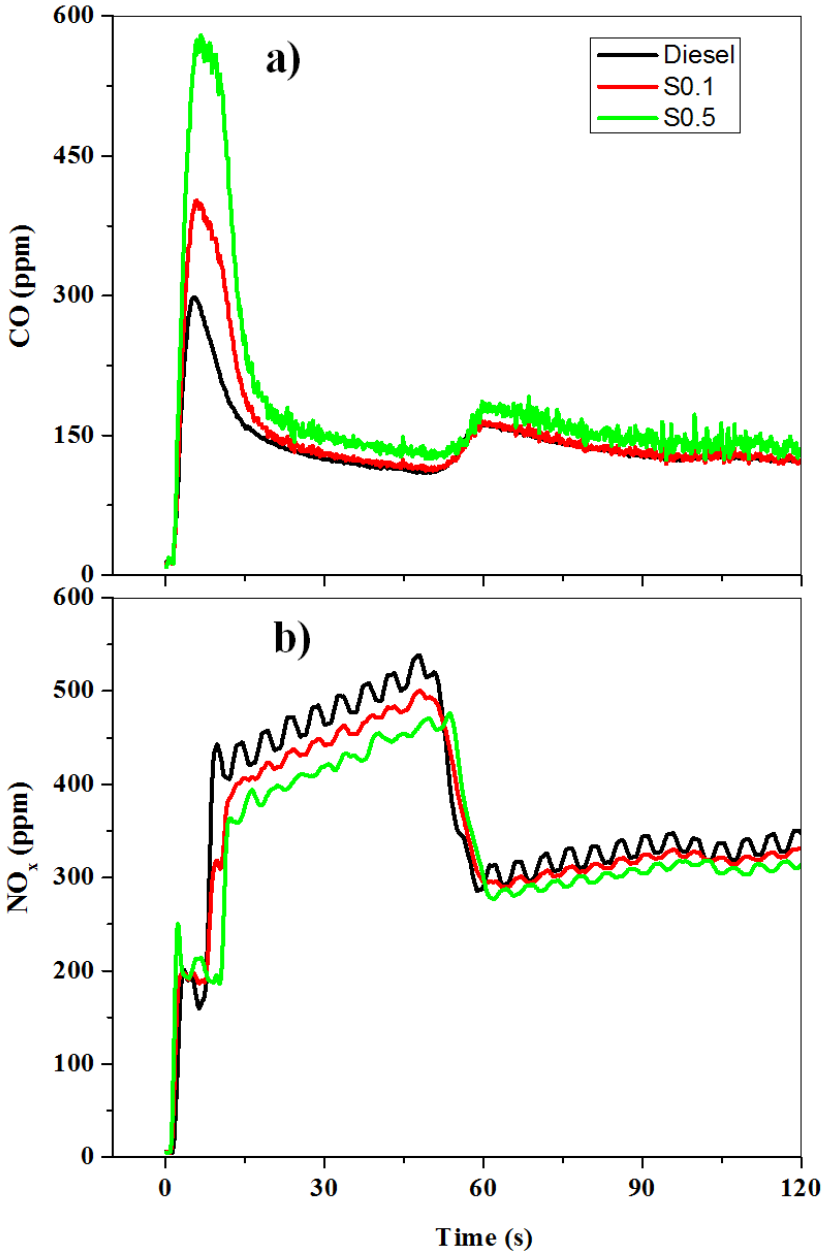

Fig. 5. a) Carbon monoxide emissions; b) Nitrogen oxide emissions during cold start for different fuels.

Fig. 6a and 6b show particle number and count median diameter in both nucleation and accumulation modes during cold start. The highest PN concentration is observed for the first 20 s during cold start period as can be seen in Fig. 6a. This PN trend is consistent with all tested fuels, but IMO compliant fuels present nearly four times higher PN emissions compared to reference diesel use. This is most likely due to low engine block temperature during cold start, which can give rise to uncompleted combustion consisting of both partially-burnt fuel and lubricant (Zare et al., 2018; Zare et al., 2017). This may cause an increase in concentrations of particle emissions. In addition, lower exhaust temperature during cold start can enhance homogeneous condensation of sulphuric acid in the exhaust flow, resulting in secondary particle formation, evident by the appearance of the nucleation mode. Particularly, IMO compliant fuels contain 0.1 and 0.5% S by mass

respectively. It can be seen clearly in Fig. 6b that particle emissions formed in the nucleation mode are dominant for IMO compliant fuels. The influence of engine injection strategy on PN emissions is not clear for the reference diesel and S0.1; however, S0.5 shows a significant impact. Single injection mode may result in a considerable increase in PN, as can be seen in Fig. 6b. This may be associated with fuel viscosity, which presents the highest value for S0.5. Fig. 6c shows the count median diameter (CMD) of particles in both the nucleation and accumulation modes. CMD of particles in the accumulation mode for all tested fuels is around 60 nm, with 10 nm for nucleation modes. Fig. 6c shows $PM_{1.0}$ concentrations during cold start. The shape of the $PM_{1.0}$ graph with CMD of particles in accumulation mode are quite similar. It may indicate the strong impact of particles in the accumulation mode on PM mass. Interestingly, injection strategy has a large effect on PM emissions. It shows the important role of the ECU in reducing engine emissions during cold start, especially on PM emissions.

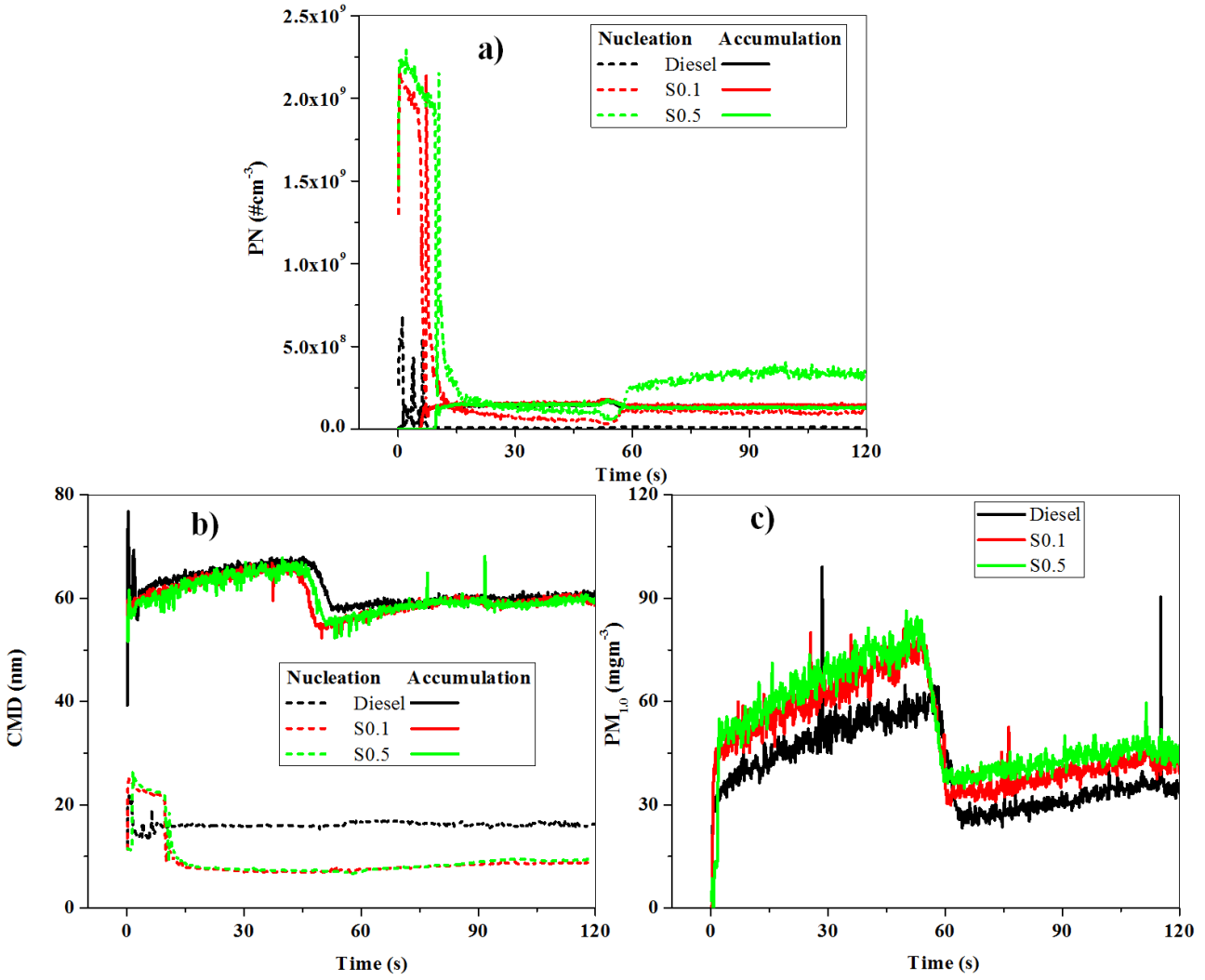

Fig. 6. a) Particle number in both nucleation and accumulation; b) Count median diameter of emitted particles both in nucleation and accumulation modes; c) $PM_{1.0}$ concentration in mg/m^3 during cold start for different fuels.

4. Conclusion

Auxiliary marine engines are predominantly used when a ship is at berth in order to generate electric power and steam. Emissions from ships at berth account for a relatively small portion of the total ship emissions; however, they possess some of the most significant health impacts on the surrounding densely-populated areas. In this study, measurements have been conducted on a marine auxiliary, heavy duty, six-cylinder, turbocharged and after-cooled diesel engine with a high pressure common rail injection system to make engine performance and emission characterisations clear during cold start. Three tested fuels were used, including a reference diesel and two IMO compliant spiked fuels. The research engine was examined at a constant speed of 1500 rpm and 25% load, under cold start. Results show that during cold start, a significant heat loss from combustion spent on heating the engine block, coolant and lubricant to overcome friction losses. Engine emissions of PN, CO, PM and NO_x during the first minute were 10, 4, 2 and 1.5 times higher than that of the second minute during the first two minutes of cold start, respectively. The ECU plays a vital role in reducing engine emissions by changing the engine injection strategy from two injections (pilot and main injection) when the engine coolant temperature is low (below 30 ºC), to single injection when the engine gets warmer. IMO compliant fuels have a higher viscosity associated with a high sulphur content resulting in an engine emissions increase during cold start. It should be taken into account that auxiliary engines running at partial load conditions during cold start considerably contribute to emissions in coastal areas. It shows a need for the use of some practical measures, such as pre-heating, before starting engines to obtain both environmental and public health advantages in coastal areas.

Acknowledgement

The first author is grateful in acknowledging the financial support received from the Government of Vietnam for a PhD scholarship. The authors would also like to acknowledge software developer, Mr. Andrew Elder from DynoLog Dynamometer Pty Ltd; laboratory assistance from Mr. Noel Hartnett; QUT staff and colleagues for their support and guidance.

Appendix A. Supplementary data

Supplementary data related to this article can be found at https://www.journals.elsevier.com/environmental-pollution/

References

Anderson, M., Salo, K., Hallquist, Å.M., Fridell, E., 2015. Characterization of particles from a marine engine operating at low loads. Atmos. Environ. 101, 65-71.

André, M., 1991. In actual use car testing: 70,000 kilometers and 10,000 trips by 55 French cars under real conditions. SAE International, Technical Paper 910039, http://doi.org/10.4271/910039.

Arumugam Sakunthalai, R., Xu, H., Liu, D., Tian, J., Wyszynski, M., Piaszyk, J., 2014. Impact of cold ambient conditions on cold start and idle emissions from diesel engines. SAE International, Technical Paper 2014-01-2715, http://doi.org/10.4271/2014-01-2715.

Bielaczyc, P., Merkisz, J., Pielecha, J., 2001. A method of reducing the exhaust emissions from DI diesel engines by the introduction of a fuel cut off system during cold start. SAE International Technical Paper 2001-01-3283, http://doi.org/10.4271/2001-01-3283.

Blasco, J., Duran-Grados, V., Hampel, M., Moreno-Gutierrez, J., 2014. Towards an integrated environmental risk assessment of emissions from ships' propulsion systems. Environ. Int. 66, 44-47.

Bodisco, T., Brown, R.J., 2013. Inter-cycle variability of in-cylinder pressure parameters in an ethanol fumigated common rail diesel engine. Energy 52, 55-65.

Bodisco, T., Low Choy, S., Brown, R.J., 2013. A Bayesian approach to the determination of ignition delay. Appl. Therm. Eng. 60, 79-87.

Cao, Y., 2007. Operation and cold start mechanisms of internal combustion engines with alternative fuels. SAE International, Technical Paper 2007-01-3609, http://doi.org/10.4271/2007-01-3609.

Chen, L., Liang, Z., Zhang, X., Shuai, S., 2017. Characterizing particulate matter emissions from GDI and PFI vehicles under transient and cold start conditions. Fuel 189, 131-140.

Chu Van, T., Ramirez, J., Rainey, T., Ristovski, Z., Brown, R.J., 2019. Global impacts of recent IMO regulations on marine fuel oil refining processes and ship emissions. Transport. Res. Part D Transp. Environ. 70, 123-134.

Chu-Van, T., Ristovski, Z., Pourkhesalian, A.M., Rainey, T., Garaniya, V., Abbassi, R., Jahangiri, S., Enshaei, H., Kam, U.S., Kimball, R., Yang, L., Zare, A., Bartlett, H., Brown, R.J., 2017. On-board measurements of particle and gaseous emissions from a large cargo vessel at different operating conditions. Environ. Pollut. 237, 832-841.

Chu-Van, T., Ristovski, Z., Surawski, N., Bodisco, T., Rahman, A.S.M., Alroe, J., Miljevic, B., Hossain, F.M., Suara, K., Rainey, T., Brown, R.J., 2018a. Effect of sulphur and vanadium spiked fuels on particle characteristics and engine performance of auxiliary diesel engines. Environ. Pollut. 243, 1943-1951, https://dx.doi.org/10.1016/j.envpol.2018.08.055.

Chu-Van, T., Surawski, N., Ristovski, Z., Yuan, C.-S., Rahman, A.S.M., Hossain, F.M., Guo, Y., Rainey, T., Brown, R.J., 2018b. The effects of diesel fuel sulphur and vanadium on engine performance and emissions. Fuel (Underreview).

Cooper, D.A., 2003. Exhaust emissions from ships at berth. Atmos. Environ. 37, 3817-3830.

Corbett, J.J., 2003. Updated emissions from ocean shipping. J. Geophys. Res. 108.

Corbett, J.J., Winebrake, J.J., Green, E.H., Kasibhatla, P., Eyring, V., Lauer, A., 2007. Mortality from ship

emissions: a global assessment. Environ. Sci. Technol. 41, 8512–8518.
Di Natale, F., Carotenuto, C., 2015. Particulate matter in marine diesel engines exhausts: emissions and control strategies. Transport. Res. Part D Transp. Environ. 40, 166-191.
Dunning, H.N., Moore, J.W., Bieber, H., Williams, R.B., 1960. Porphyrin, nickel, vanadium, and nitrogen in petroleum. J. Chem. Eng. Data 5, 546-549.
Eyring, V., 2005. Emissions from international shipping: 2. Impact of future technologies on scenarios until 2050. J. Geophys. Res. 110.
Eyring, V., Isaksen, I.S.A., Berntsen, T., Collins, W.J., Corbett, J.J., Endresen, O., Grainger, R.G., Moldanova, J., Schlager, H., Stevenson, D.S., 2010. Transport impacts on atmosphere and climate: shipping. Atmos. Environ. 44, 4735-4771.
Hossain, F.M., Nabi, M.N., Rainey, T.J., Bodisco, T., Rahman, M.M., Suara, K., Rahman, S.M.A., Chu-Van, T., Ristovski, Z., Brown, R.J., 2017. Investigation of microalgae HTL fuel effects on diesel engine performance and exhaust emissions using surrogate fuels. Energy Convers. Manag. 152, 186-200.
IMO, 1997. International Convention for the Prevention of Pollution from Ships MARPOL 73/78: the Regulations for the Prevention of Air Pollution from Ships (Annex VI). The International Maritime Organization (IMO), London.
IMO, 2009. Second IMO GHG Study 2009. The International Maritime Organization (IMO), London.
Mitchell, B.J., Zare, A., Bodisco, T.A., Nabi, M.N., Hossain, F.M., Ristovski, Z.D., Brown, R.J., 2017. Engine blow-by with oxygenated fuels: a comparative study into cold and hot start operation. Energy 140, 612-624.
Mueller, L., Jakobi, G., Czech, H., Stengel, B., Orasche, J., Arteaga-Salas, J.M., Karg, E., Elsasser, M., Sippula, O., Streibel, T., Slowik, J.G., Prevot, A.S.H., Jokiniemi, J., Rabe, R., Harndorf, H., Michalke, B., Schnelle-Kreis, J., Zimmermann, R., 2015. Characteristics and temporal evolution of particulate emissions from a ship diesel engine. Appl. Energy 155, 204-217.
Reda, A.A., Schnelle-Kreis, J., Orasche, J., Abbaszade, G., Lintelmann, J., Arteaga-Salas, J.M., Stengel, B., Rabe, R., Harndorf, H., Sippula, O., Streibel, T., Zimmermann, R., 2015. Gas phase carbonyl compounds in ship emissions: differences between diesel fuel and heavy fuel oil operation. Atmos. Environ. 112, 370-380.
Reiter, M.S., Kockelman, K.M., 2016. The problem of cold starts: a closer look at mobile source emissions levels. Transport. Res. Part D Transp. Environ. 43, 123-132.
Ristovski, Z.D., Miljevic, B., Surawski, N.C., Morawska, L., Fong, K.M., Goh, F., Yang, I.A., 2012. Respiratory health effects of diesel particulate matter. Respirology 17, 201-212.
Roberts, A., Brooks, R., Shipway, P., 2014. Internal combustion engine cold start efficiency: a review of the problem, causes and potential solutions. Energy Convers. Manage. 82, 327-350.
Saiyasitpanich, P., Lu, M., Keener, T.C., Liang, F., Khang, S.J., 2005. The effect of diesel fuel sulfur content on particulate matter emissions for a nonroad diesel generator. J. Air Waste Manage. Assoc. 55, 993-998.
Samhaber, C., Wimmer, A., Loibner, E., 2001. Modeling of engine warm-up with integration of vehicle and engine cycle simulation. SAE International, Technical Paper 2001-01-1697,

http://doi.org/10.4271/2001-01-1697.

Sofiev, M., Winebrake, J.J., Johansson, L., Carr, E.W., Prank, M., Soares, J., Vira, J., Kouznetsov, R., Jalkanen, J.-P., Corbett, J.J., 2018. Cleaner fuels for ships provide public health benefits with climate tradeoffs. Nat. Commun. 9, 406.

Surawski, N.C., Miljevic, B., Bodisco, T.A., Situ, R., Brown, R.J., Ristovski, Z.D., 2014. Performance and gaseous and particle emissions from a liquefied petroleum gas (LPG) fumigated compression ignition engine. Fuel 133, 17-25.

United Nations, 2017. Review of Maritime Transport 2017. United Nations, Switzerland, https://unctad.org/en/PublicationsLibrary/rmt2017_en.pdf.

Will, F., Boretti, A., 2011. A new method to warm up lubricating oil to improve the fuel efficiency during cold start. SAE Int. J. Engines 4, 175-187, http://doi.org/10.4271/2011-01-0318.

Winnes, H., Fridell, E., 2010. Emissions of NO_X and particles from manoeuvring ships. Transport. Res. Part D Transp. Environ. 15, 204-211.

Winnes, H., Moldanová, J., Anderson, M., Fridell, E., 2016. On-board measurements of particle emissions from marine engines using fuels with different sulphur content. Proc. Inst. Mech. Eng. Part M J. Eng. Marit. Environ. 230, 45-54.

Zare, A., Bodisco, T.A., Nabi, M.N., Hossain, F.M., Ristovski, Z.D., Brown, R.J., 2018. A comparative investigation into cold start and hot start operation of diesel engine performance with oxygenated fuels during transient and steady-state operation. Fuel 228, 390-404.

Zare, A., Nabi, M.N., Bodisco, T.A., Hossain, F.M., Rahman, M.M., Chu Van, T., Ristovski, Z.D., Brown, R.J., 2017. Diesel engine emissions with oxygenated fuels: a comparative study into cold start and hot start operation. J. Clean. Prod. 162, 997-1008.

Zhang, Z.-H., Balasubramanian, R., 2017. Effects of cerium oxide and ferrocene nanoparticles addition as fuel-borne catalysts on diesel engine particulate emissions: environmental and health implications. Environ. Sci. Technol. 51, 4248-4258.